Extension of the CVBEM to higher-order trial functions

T. V. Hromadka II and C. C. Yen

Williamson and Schmid, Irvine, CA 92714, USA
(Received October 1987; revised January 1988)

The higher-order trial functions, such as the parabolic, cubic, and Hermite cubic polynomial functions, for the complex boundary element method are derived and their computer programs are developed. Using the considered higher-order trial function, models obtained compatible results to the linear trial function model.

Keywords: complex variables, trail functions, error analysis, approximate boundary

Introduction

The main purpose of this paper is to summarize the results of recent research involving the implementation of higher-order trial functions (used for interpolation purposes) into the boundary integral equation formulation known as the complex variable boundary element method (CVBEM). The main thrust of this research was to (1) develop the nodal point equations based on the CVBEM technique for solving two-dimensional boundary value problems of the Poisson equation (e.g., $\nabla^2\phi = f(x,y)$), where parabolic, cubic, and Hermite cubic polynomial trial functions are used, and (2) develop computer programs based on each of the new formulations, and examine whether a significant improvement in computational efficiency is provided (over the standard linear trial function) by use of any of the considered techniques. This paper focuses upon the first objective, whereas the second objective is summarized by the example problem results included herein.

Because a thorough literature review and mathematical development of the CVBEM is contained in the book by Hromadka,[1] only the key equations needed to formulate each of the nodal point equations are provided in this paper. Discussions as to the usability of the CVBEM in engineering analysis, and the convenient error analysis techniques provided by the CVBEM, are found in Ref. 1.

Nodal point equations are developed for the principal value of the Cauchy integral for the linear, parabola, cubic, and Hermite cubic polynomial trial functions. Because of the lengthy derivations, only the final equation forms (which would be used in a computer program) are presented. Detailed derivations involved in the linear trial function CVBEM model can be found in Hromadka,[1] and each of the higher-order trial function derivations follow similar mathematical steps in their respective derivations of the nodal point equations.

Boundary integral equation formulation—linear trial function approximation

Consider a simply connected domain Ω with a simple closed contour boundary Γ, as shown in *Figure 1*. The boundary can be subdivided into m boundary elements Γ_j such that

$$\Gamma = \bigcup_{j=1}^{m} \Gamma_j \tag{1}$$

On each boundary element, define two nodal points located at the element endpoints; for element j, the coordinates of the nodes are z_j and z_{j+1}. A simple linear trial function $\alpha(s)$ is assumed on each element such that

$$\alpha(s) = \bar{\omega}_j s + \bar{\omega}_{j+1}(1 - s) \qquad 0 \le s \le 1 \tag{2}$$

where $\bar{\omega}_j$ is the complex nodal value for node j, and where $\bar{\omega}_j = \bar{\phi}_j + i\bar{\psi}_j$. In equation (2), $\bar{\phi}_j$ and $\bar{\psi}_j$ are state variable and stream function nodal values at coordinate z_j.

The CVBEM utilizes an integral function $\hat{\omega}(z)$ defined by

$$2\pi i\hat{\omega}(z) = \sum_{j=1}^{m} \int_{\Gamma_j} \left(\frac{\alpha(\zeta)\, d\zeta}{\zeta - z} \right)_j \qquad z \in \Omega \quad z \notin \Gamma \tag{3}$$

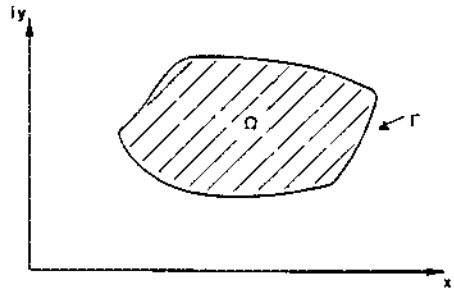

Figure 1 Problem domain Ω with boundary Γ

where ζ is the complex variable of integration, $\alpha(\zeta)$ are the continuous trial functions, and the subscript j refers to element contour Γ_j. Because the $\alpha(\zeta)$ are continuous on Γ_j, the approximation function $\hat{\omega}(z)$ is analytic for all z in the interior of Γ.

Equation (3) can be evaluated for any point z interior of Γ by noting that

$$\int_{\Gamma_j} \frac{\alpha(\zeta)\,d\zeta}{\zeta - z} = \bar{\omega}_{j+1}\left[1 + \left(\frac{z - z_j}{z_{j+1} - z_j}\right) H_j\right] - \bar{\omega}_j\left[1 + \left(\frac{z - z_{j+1}}{z_{j+1} - z_j}\right) H_j\right] \quad (4)$$

where

$$H_j = \ln\left(\frac{z_{j+1} - z}{z_j - z}\right)$$

A boundary integral equation can be formulated for each nodal point by

$$2\pi i\hat{\omega}(z_1) = \lim_{z \to z_1} \sum_{j=1}^{m} \int_{\Gamma_j} \left(\frac{\alpha(\zeta)\,d\zeta}{\zeta - z}\right)_j \quad (5)$$

where the limit is evaluated as z approaches arbitrary nodal coordinate z_1 from the interior of Γ. Substituting equation (4) into equation (5), we get[2]

$$2\pi i\hat{\omega}(z_1) = \bar{\omega}_1 H_1 + \sum_{j=2}^{m-1}\left[\bar{\omega}_{j+1}\left(\frac{z_1 - z_j}{z_{j+1} - z_j}\right) - \bar{\omega}_j\left(\frac{z_1 - z_{j+1}}{z_{j+1} - z_j}\right)\right] H_j \quad (6)$$

where

$$H_j = \ln\left(\frac{d(j+1,1)}{d(j,1)}\right) + i\theta(j+1,j) \quad (7)$$

and

$$H_1 = \ln\left(\frac{d(2,1)}{d(m,1)}\right) + i\theta(2,m)$$

In equation (7), $d(j+1,1)$ is the distance between nodal coordinates z_{j+1} and z_1, and $\theta(j+1,j)$ is the angle between coordinates z_{j+1} and z_j (*Figure 2*). Additionally, $\theta(2,m)$ is the vertex exterior angle shown in *Figure 2*.

An examination of the approximation function definition of equation (6) reveals that $\hat{\omega}(z_1)$ is a function of the boundary geometry and nodal values $\bar{\omega}_j$. Generally, $\hat{\omega}(z)$ is not the desired solution of $\omega(z) = \phi + i\psi$, and $\hat{\omega}(z_j) \neq \bar{\omega}(z_j)$.

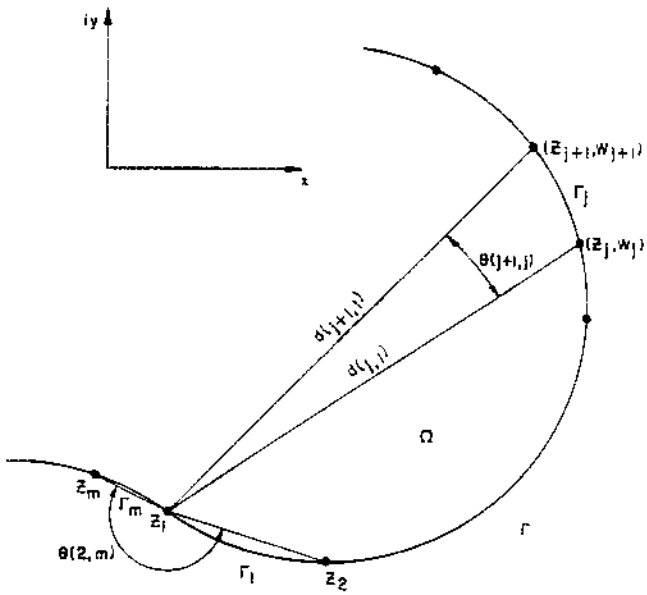

Figure 2 CVBEM linear trial function geometry

CVBEM model development

The CVBEM formulation results in a matrix system which depends on the trial function definition. Because of the direct analogy, the linear trial function formulation is used in the following to describe the matrix system development. The other trial functions considered here also result in similar matrix system mechanics.

The nodal values $\bar{\omega}_j$ are composed of two components $\bar{\omega}_j = \bar{\phi}_j + i\bar{\psi}_j$, where either $\bar{\phi}$ or $\bar{\psi}$ is known at each z_j by the given boundary condition definitions. Consequently, each nodal point has an assigned known boundary value and a corresponding unknown boundary value. Should both boundary nodal values be known at each z_j, then the approximation function $\hat{\omega}(z)$ is defined throughout the interior of Γ. Therefore, in order to calculate $\hat{\omega}(z_j)$ values, we need estimates of the unknown nodal boundary condition values. In the following discussion, it is assumed that $\bar{\phi}_j$ is specified at each z_j ($\bar{\phi}_j = \phi_j$) and that the $\bar{\psi}_j$ are unknown (except for a single nodal point value where the constant of integration is evaluated). The discussion is immediately extendable to mixed boundary conditions. The following notation is used for the three sets of nodal point values:

$\omega_j = \omega(z_j) = \phi_j + i\psi_j$	exact solution of boundary value problem solution at node j
$\bar{\omega}_j = \bar{\phi}_j + i\bar{\psi}_j$	boundary condition nodal values

$\hat{\omega}_j = \hat{\phi}_j + i\hat{\psi}_j$ approximation values at node j

Application of equation (6) for each nodal point results in m linear equations, which can be written in matrix form as

$$\hat{\boldsymbol{\omega}} = \mathbf{C}_R(\bar{\boldsymbol{\phi}},\bar{\boldsymbol{\psi}}) + i\mathbf{C}_I(\bar{\boldsymbol{\phi}},\bar{\boldsymbol{\psi}}) \tag{8}$$

where $\mathbf{C}_R$ and $\mathbf{C}_I$ are $m \times 2m$ matrices of real constants representing the real and imaginary parts of the boundary integral equations, respectively. From (8), two matrix systems require simultaneous solution.

$$\hat{\boldsymbol{\phi}} = \mathbf{C}_R(\bar{\boldsymbol{\phi}},\bar{\boldsymbol{\psi}}) \qquad \hat{\boldsymbol{\psi}} = \mathbf{C}_I(\bar{\boldsymbol{\phi}},\bar{\boldsymbol{\psi}}) \tag{9}$$

where $(\bar{\boldsymbol{\phi}},\bar{\boldsymbol{\psi}})$ is the array of nodal point boundary values.

One method of solving equation (9) is to set $\hat{\boldsymbol{\psi}} = \bar{\boldsymbol{\psi}}$ and solve

$$\bar{\boldsymbol{\psi}} = \mathbf{C}_I(\bar{\boldsymbol{\phi}},\bar{\boldsymbol{\psi}}) \tag{10}$$

using the known $\bar{\boldsymbol{\phi}}$, followed by the solution of $\hat{\boldsymbol{\phi}} = \mathbf{C}_R(\bar{\boldsymbol{\phi}},\bar{\boldsymbol{\psi}})$, which results in values for $\bar{\boldsymbol{\psi}}$. Note that the calculation of $\bar{\boldsymbol{\psi}}$ can also be achieved by solving

$$\bar{\boldsymbol{\phi}} = \mathbf{C}_R(\bar{\boldsymbol{\phi}},\bar{\boldsymbol{\psi}}) \tag{11}$$

One may use equation (11) due to the approximator $\hat{\boldsymbol{\omega}}(z)$ matching the boundary condition values at each nodal point, and then evaluate the relative error of $\boldsymbol{\omega} - \hat{\boldsymbol{\omega}}$ by analysis of $\bar{\boldsymbol{\psi}} - \hat{\boldsymbol{\psi}}$ and $\boldsymbol{\phi} - \hat{\boldsymbol{\phi}}$ on Γ. However, $\bar{\boldsymbol{\psi}} - \hat{\boldsymbol{\psi}}$ is not known continuously on Γ. (Recall that, for simplicity, a Dirichlet problem is being considered for development purposes. The case of a mixed boundary value problem follows analogously.) Should the model of equation (10) be used, evaluation of the relative error of $\boldsymbol{\psi} - \hat{\boldsymbol{\psi}}$ is aided by $\bar{\boldsymbol{\psi}} = \hat{\boldsymbol{\psi}}$, and $\boldsymbol{\phi} - \hat{\boldsymbol{\phi}}$ is known continuously on Γ.

CVBEM model: parabola trial function

The parabolic trial function is derived by using the second-order Lagrange interpolating polynomials over the boundary elements. A boundary element consists of three colinear points z_j, z_{j+1}, z_{j+2}, where z_{j+1} is not necessarily equidistant between z_j and z_{j+2} (see *Figure 3*).

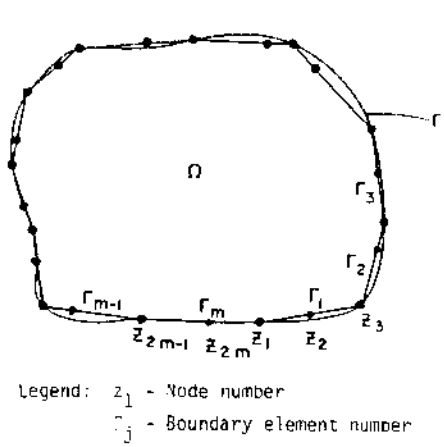

Figure 3 Nodes and boundary elements for parabola trial function

For point z on a boundary element,

$$N_1(z) = \frac{(z - z_{j+1})(z - z_{j+2})}{(z_j - z_{j+1})(z_j - z_{j+2})} = \frac{z^2 - z(z_{j+1} + z_{j+2}) + z_{j+1}z_{j+2}}{(z_j - z_{j+1})(z_j - z_{j+2})} \tag{12}$$

or, in polynomial form,

$$N_1(z) = a_1z^2 + b_1z + c_1 \tag{13}$$

where

$$a_1 = \frac{1}{(z_j - z_{j+1})(z_j - z_{j+2})}$$

$$b_1 = \frac{-(z_{j+1} + z_{j+2})}{(z_j - z_{j+1})(z_j - z_{j+2})}$$

$$c_1 = \frac{z_{j+1}z_{j+2}}{(z_j - z_{j+1})(z_j - z_{j+2})}$$

For $N_2(z)$,

$$N_2(z) = a_2z^2 + b_2z + c_2 \tag{14}$$

where

$$a_2 = \frac{1}{(z_{j+1} - z_j)(z_{j+1} - z_{j+2})}$$

$$b_2 = \frac{-(z_{j+1} + z_{j+2})}{(z_{j+1} - z_j)(z_{j+1} - z_{j+2})}$$

$$c_2 = \frac{z_{j+1}z_{j+2}}{(z_{j+1} - z_j)(z_{j+1} - z_{j+2})}$$

and for $N_3(z)$,

$$N_3(z) = a_3z^2 + b_3z + c_3 \tag{15}$$

where

$$a_3 = \frac{1}{(z_{j+2} - z_j)(z_{j+2} - z_{j-2})}$$

$$b_3 = \frac{-(z_j + z_{j+1})}{(z_{j+2} - z_j)(z_{j-2} - z_{j+1})}$$

$$c_3 = \frac{z_jz_{j+1}}{(z_{j-2} - z_j)(z_{j+2} - z_{j+1})}$$

For boundary element Γ_j, equation (3) is now written as

$$\int_{\Gamma_j} \left(\frac{\alpha(\zeta)\,d\zeta}{\zeta - z}\right)_j = \int_{\Gamma_j} \frac{\sum_{i=1}^{3} N_{ij}(\zeta)\bar{\omega}_{ij}\,d\zeta}{\zeta - z} \tag{16}$$

where the following integration holds for all three basic

functions:

$$\int_{\Gamma_j} \frac{(a\zeta^2 + b\zeta + c)\,d\zeta}{\zeta - z_0} = \int_{\Gamma_j} \frac{a\zeta^2\,d\zeta}{\zeta - z_0} + \int_{\Gamma_j} \frac{b\zeta\,d\zeta}{\zeta - z_0} + \int_{\Gamma_j} \frac{c\,d\zeta}{\zeta - z_0} \quad (17)$$

For z_0 not a nodal point,

$$\begin{aligned}\int_{\Gamma_j} \frac{\alpha(\zeta)\,d\zeta}{\zeta - z_0} = {} & \bar{\omega}_{1,j}(z)\left((a_1 z_0^2 + b_1 z_0 + c_1)\left(\ln\left(\frac{z_{j+2} - z_0}{z_j - z_0}\right) + i(2\pi - \theta)\right) + (a_1 z_0 + b_1)(z_{j+2} - z_j) + \frac{a_1}{2}(z_{j+2}^2 - z_j^2)\right) \\ & + \bar{\omega}_{2,j}(z)\left((a_2 z_0^2 + b_2 z_0 + c_2)\left(\ln\left(\frac{z_{j+2} - z_0}{z_j - z_0}\right) + i(2\pi - \theta)\right) + (a_2 z_0 + b_2)(z_{j+2} - z_j) + \frac{a_2}{2}(z_{j+2}^2 - z_j^2)\right) \\ & + \bar{\omega}_{3,j}(z)\left((a_3 z_0^2 + b_3 z_0 + c_3)\left(\ln\left(\frac{z_{j+2} - z_0}{z_j - z_0}\right) + i(2\pi - \theta)\right) + (a_3 z_0 + b_3)(z_{j+2} - z_j) + \frac{a_3}{2}(z_{j+2}^2 - z_j^2)\right)\end{aligned} \quad (18)$$

Principal value calculations and matrix development

When principal value contributions for a nodal point z_0 are calculated, two categories of nodal points must be taken into consideration: (1) z_0 is an endpoint of the boundary element; or (2) z_0 is an interior point. Consider z_0 as node 1, and denote it as $z_{1,1}$ and $z_{3,m}$, where, in general, $z_{i,j}$ is the ith node of the jth boundary element. The angle θ_j is the angle between $z_{1,1}$ and the endpoints of boundary element j. The nodal point convention used with this trial function is shown in *Figure 4*.

The boundary integral approximation equation in this case is

$$\begin{aligned}2\pi i\omega(z_{1,1}) \cong {} & \bar{\omega}_{1,1}\left((a_{1,1}z_{1,1}^2 + b_{1,1}z_{1,1} + c_{1,1} + z_{1,1}^2 + b_{3,m}z_{1,1} + c_{3,m})\left(\ln\left(\frac{z_{3,1} - z_{1,1}}{z_{1,m} - z_{1,1}}\right) + i(2\pi - \theta_{1,m})\right)\right. \\ & \left. + \frac{z_{3,1}^2 - z_{1,1}^2}{2} + \frac{z_{3,1}^2 - z_{1,1}^2}{2} + (z_{1,1} + b_{1,1})(z_{3,1} - z_{1,1}) + (z_{1,1} + b_{3,m})(z_{1,1} - z_{1,m})\right) \\ & + \sum_{i=2}^{3} \bar{\omega}_{i,1}\left((a_{i,1}z_{1,1}^2 + b_{i,1}z_{1,1} + c_{i,1})\left(\ln\left(\frac{z_{3,1} - z_{1,1}}{z_{1,m} - z_{1,1}}\right) + i(2\pi - \theta_{1,m})\right) + \frac{z_{3,1}^2 - z_{1,1}^2}{2} + (z_{1,1} + b_{i,1})(z_{3,1} - z_{1,1})\right) \quad (19) \\ & + \sum_{i=1}^{3} \bar{\omega}_{i,m}\left((a_{i,m}z_{1,1}^2 + b_{i,m}z_{1,1} + c_{i,m})\left(\ln\left(\frac{z_{3,1} - z_{1,1}}{z_{1,m} - z_{1,1}}\right) + i(2\pi - \theta_{1,m})\right) + \frac{z_{1,1}^2 - z_{1,m}^2}{2} + (z_{1,1} + b_{i,m})(z_{1,1} - z_{1,m})\right) \\ & + \sum_{j=2}^{m}\sum_{i=1}^{3} \bar{\omega}_{i,j}\left((a_{i,j}z_{1,1}^2 + b_{i,j}z_{1,1} + c_{i,j})\left(\ln\left(\frac{z_{3,j} - z_{1,1}}{z_{1,j} - z_{1,1}}\right) + i(2\pi - \theta_j)\right) + \frac{z_{3,j}^2 - z_{1,j}^2}{2} + (z_{1,1} + b_{i,j})(z_{3,j} - z_{1,j})\right)\end{aligned}$$

Now consider $z_0 = z_{2,1}$, which is an interior point of the boundary element. The following equations are used:

$$\begin{aligned}2\pi i\omega(z_{2,1}) = {} & \bar{\omega}_{2,1}\left((a_{2,1}z_{2,1}^2 + b_{2,1}z_{2,1} + c_{2,1})\left(\ln\left(\frac{z_{3,1} - z_{2,1}}{z_{1,1} - z_{2,1}}\right) + i(2\pi - \theta_{1,m})\right) + \frac{z_{3,1}^2 - z_{1,1}^2}{2} + (z_{2,1} + b_{2,1})(z_{3,1} - z_{1,1})\right) \\ & + \sum_{i=1}^{3} \bar{\omega}_{i,1}\left((a_{i,1}z_{2,1}^2 + b_{i,1}z_{2,1} + c_{i,1})\left(\ln\left(\frac{z_{3,1} - z_{2,1}}{z_{1,1} - z_{2,1}}\right) + i(2\pi - \theta_{1,m})\right) + \frac{z_{3,1}^2 - z_{1,1}^2}{2} + (z_{2,1} + b_{i,1})(z_{3,1} - z_{1,1})\right) \quad (20) \\ & + \sum_{j=2}^{m}\sum_{i=1}^{3} \bar{\omega}_{i,j}\left((a_{i,j}z_{2,1}^2 + b_{i,j}z_{2,1} + c_{i,j})\left(\ln\left(\frac{z_{3,j} - z_{2,1}}{z_{1,j} - z_{2,1}}\right) + i(2\pi - \theta_j)\right) + \frac{z_{3,j}^2 - z_{1,j}^2}{2} + (z_{2,1} + b_{i,j})(z_{3,j} - z_{1,j})\right)\end{aligned}$$

CVBEM model: cubic trial function

Analogous to the previous model developments, let Γ be discretized into m boundary elements, Γ_j, $\Gamma = \cup_{j=1}^{m} \Gamma_j$, where $\Gamma_j \cap \Gamma_{j+1} = z_j \in \Gamma$. Let each boundary element Γ_j be further discretized into three segments so that there are four interpolation points on each boundary element. (This compares to having three interpolation points for the parabolic trial function, as shown in *Figure 4*.)

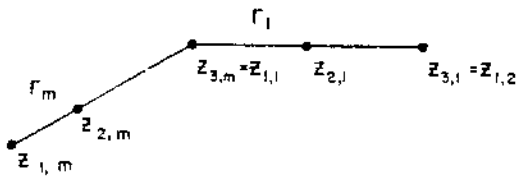

Figure 4 Nodal point naming convention

The cubic basis function on each Γ_j determines a continuous global trial function on Γ by

$$\sum_{j=1}^{m} (\alpha(\zeta))_j = \sum_{j=1}^{m} (N_{j,1}\bar{\omega}_{j,1} + N_{j,2}\bar{\omega}_{j,2} + N_{j,3}\bar{\omega}_{j,3} + N_{j,4}\bar{\omega}_{j,4}) = \sum_{j=1}^{m}\sum_{k=1}^{4} N_{j,k}\bar{\omega}_{j,k} \tag{21}$$

where

$$N_{j,1}(\zeta) = \begin{cases} \prod_{\substack{k=1 \\ k\neq i}}^{4} \dfrac{\zeta - z_{j,k}}{z_{i,k} - z_{j,k}} & \zeta \in \Gamma_j \\ 0 & \zeta \notin \Gamma_j \end{cases} \tag{22}$$

The point $z_{j,i}$ represents the jth interpolation point of the ith boundary element. Also $z_{j,2}$ and $z_{j,3}$ are spaced between $z_{j,1}$ and $z_{j,4}$, where $z_{j,1} = z_j$ and $z_{j,4} = z_{j+1}$.

The contribution from each boundary element Γ_j can be calculated by

$$\begin{aligned} \int_{\Gamma_j} \frac{\alpha(\zeta)\,d\zeta}{\zeta - z} &= \sum_{i=1}^{4} \int_{\Gamma_j} \frac{N_{j,i}(\xi)\bar{\omega}_{j,i}(\xi)}{\xi - z_0} d\xi \\ &= \sum_{i=1}^{4} \int_{\Gamma_j} \frac{\bar{\omega}_{j,i}(a_{ji0} + a_{ji1}\xi + a_{ji2}\xi^2 + a_{ji3}\xi^3)}{\xi - z} d\xi \\ &= \sum_{i=1}^{4} \int_{\Gamma} \left[\bar{\omega}_{j,i}a_{ji3}\xi^2 + \bar{\omega}_{j,1}(a_{ji2} + za_{ji3})\xi \right. \\ &\quad + \bar{\omega}_{j,i}(a_{ji1} + za_{ji2} + z^2a_{ji3}) \\ &\quad \left. + \frac{a_{ji0} + za_{ji1} + z^2a_{ji2} + z^3a_{ji3}}{\xi - z} \right] d\xi \end{aligned} \tag{23}$$

In summation notation,

$$\int_{\Gamma_j} \frac{\alpha(\zeta)\,d\zeta}{\zeta - z} = \sum_{i=1}^{4} \bar{\omega}_{j,i} \frac{a_{ji3}}{3} (z_{j,4}^3 - z_{j,1}^3) \tag{24}$$

The a_{ijk} variables are obtained by multiplying out the Lagrangian polynomial for the jth position: $L_{ij}(z) = a_{ij0} + a_{ij1}z + a_{ij2}z^2 + a_{ij3}z^3$. For example,

$$\begin{aligned} a_{113} &= \frac{1}{(z - z_1)(z - z_2)(z - z_3)} \\ a_{112} &= \frac{-z_1 - z_2 - z_3}{(z - z_1)(z - z_2)(z - z_3)} \\ a_{111} &= \frac{z_1z_2 + z_2z_3 + z_3z_1}{(z - z_1)(z - z_2)(z - z_3)} \\ a_{110} &= \frac{-z_1z_2z_3}{(z - z_1)(z - z_2)(z - z_3)} \end{aligned} \tag{25}$$

Principal value calculations and matrix development follow the previous linear and quadratic model presentations.

CVBEM model: Hermite (cubic) trial functions

In the Hermite set of basis functions, the derivative terms are utilized, so principal value calculations differ from the previous developments.

Since the values of the analytic functions $w(z)$ and its derivatives $w'(z)$ are utilized at the nodal points, and we desire a cubic approximation, then define a continuous trial function on Γ_j by

$$\alpha(\zeta) = \sum_{j=1}^{n} P_j(\zeta) \tag{26}$$

$$\alpha'(\zeta) = \sum_{j=1}^{n} P_j'(\zeta) \tag{27}$$

where $\alpha(\zeta)$ is defined as

$$\alpha(\zeta) = a_j + b_j\zeta + c_j\zeta^2 + d_j\zeta^3 \tag{28}$$

and the derivative $\alpha'(\zeta)$ is

$$\alpha'(\zeta) = b_j + 2c_j\zeta + 3d_j\zeta^2 \tag{29}$$

Collocating at the nodal points, we have four equations in four unknowns, which we solve to obtain the coefficients. Upon rearranging the coefficients, we get new expressions for $\alpha(z)$ and $\alpha'(z)$ at point z:

$$\begin{aligned} \alpha(z) = {} & \bar{\omega}_j(Z_{2j})^2(1 + 2Z_{1j}) + \bar{\omega}_{j+1}(Z_{1j})^2(1 + 2Z_{2j}) \\ & + \bar{\omega}_j'Z_{1j}Z_{2j}(z_{j+1} - z) + \bar{\omega}_{j+1}'Z_{1j}Z_{2j}(z_j - z) \end{aligned} \tag{30}$$

$$\begin{aligned} \alpha'(z) = {} & \bar{\omega}_jZ_{1j}Z_{2j}\left(\frac{6}{z_j - z_{j+1}}\right) \\ & + \bar{\omega}_{j+1}Z_{1j}Z_{2j}\left(\frac{6}{z_{j+1} - z_j}\right) \\ & + \bar{\omega}_j'Z_{2j}(1 - 3Z_{1j}) \\ & + \bar{\omega}_{j+1}'Z_{1j}(1 - 3Z_{2j}) \end{aligned} \tag{31}$$

where Z_{1j} and Z_{2j} are defined as

$$Z_{1j} = \frac{z - z_j}{z_{j+1} - z_j} \qquad Z_{2j} = \frac{z_{j+1} - z}{z_{j+1} - z_j}$$

Principal value calculations

Since we desire the value of the approximation functions on the boundary Γ as well as the interior of Ω, we must consider the following equations:

$$\hat{\omega}(z) \cong \frac{1}{2\pi i}\sum_{j=1}^{n}\lim_{z_0\to z}\int_{\Gamma_j}\frac{P_j(\zeta)}{\zeta - z_0}\,d\zeta \tag{32}$$

$$\hat{\omega}'(z) \cong \frac{1}{2\pi i}\sum_{j=1}^{n}\lim_{z_0\to z}\int_{\Gamma_j}\frac{P_j(\zeta)}{(\zeta - z_0)}\,d\zeta \tag{33}$$

Simplifying the last integrals gives

$$\begin{aligned}\hat{\omega}(z) \cong{}& \frac{1}{2\pi i}\lim_{z_0\to z}\sum_{j=1}^{n}P_j(z)\ln\frac{z_{j+1}-z_0}{z_j-z_0}\\ &+\frac{1}{2\pi i}2\sum_{j=1}^{n}(\bar{\omega}_{j+1}-\bar{\omega}_j)Z_{1j}Z_{2j}\\ &+\frac{1}{2\pi i}\frac{1}{3}\sum_{j=1}^{n}\frac{\bar{\omega}'_{j+1}+\bar{\omega}'_j}{z_{j+1}-z_j}(z_{j+1}^2+z_{j+1}z_j)\\ &+\frac{1}{2\pi i}\frac{1}{3}\sum_{j=1}^{n}\frac{\bar{\omega}'_{j+1}+\bar{\omega}'_j}{z_{j+1}-z_j}(z_j^2-3z_{j+1}z)\\ &+\frac{1}{2\pi i}\frac{1}{3}\sum_{j=1}^{n}\frac{\bar{\omega}'_{j+1}+\bar{\omega}'_j}{z_{j+1}-z_j}(3z^2-3z_jz)\end{aligned} \tag{34}$$

$$\begin{aligned}\hat{\omega}'(z) \cong{}& \frac{1}{2\pi i}\lim_{z_0\to z}\sum_{j=1}^{n}P'_j(z)\ln\frac{z_{j+1}-z_0}{z_j-z_0}\\ &+\frac{1}{2\pi i}3\sum_{j=1}^{n}\frac{z_{j+1}-z_j-2z}{z_{j+1}-z_j}\frac{\bar{\omega}_{j+1}-\bar{\omega}_j}{z_{j+1}-z_j}\\ &-\frac{1}{2\pi i}3\sum_{j=1}^{n}\frac{z_{j+1}-z_j-2z}{z_{j+1}-z_j}\frac{\bar{\omega}'_{j+1}}{2}\\ &-\frac{1}{2\pi i}3\sum_{j=1}^{n}\frac{z_{j+1}-z_j-2z}{z_{j+1}-z_j}\frac{\bar{\omega}'_j}{2}\end{aligned} \tag{35}$$

which are valid for $z \in \Omega$.

The terms involving logarithms in (34) and (35) are simplified as

$$\begin{aligned}&\lim_{z_0\to z_k}\sum_{j=1}^{n}P_j(z_k)\ln\frac{z_{j+1}-z_0}{z_j-z_0}\\ &\quad=\sum_{j=1,\neq k,k-1}^{n}P_j(z_k)\ln\frac{z_{j+1}-z_k}{z_j-z_k}\\ &\qquad+\bar{\omega}_k\ln\frac{z_{k+1}-z_k}{z_{k-1}-z_k}\end{aligned} \tag{36}$$

$$\begin{aligned}&\lim_{z_0\to z_k}\sum_{j=1}^{n}P'_j(z_k)\ln\frac{z_{j+1}-z_0}{z_j-z_0}\\ &\quad=\sum_{j=1,\neq k,k-1}^{n}P'_j(z_k)\ln\frac{z_{j+1}-z_k}{z_j-z_k}\\ &\qquad+\bar{\omega}'_k\ln\frac{z_{k+1}-z_k}{z_{k-1}-z_k}\end{aligned} \tag{37}$$

where z_k is a nodal point of Γ and $z_0 = z_n$, $z_{n+1} = z_1$.

Matrix development

To implement the Hermite CVBEM, we simplify the equations from the above development to obtain

$$\begin{aligned}\bar{\omega}_k \cong{}& \frac{1}{2\pi i}\sum_{j=1}^{n}(\bar{\omega}_{j-1}cc1jk-\bar{\omega}_jcc1jk)\\ &+\frac{1}{2\pi i}\sum_{j=1}^{n}(\bar{\omega}'_{j+1}cc2jk+\bar{\omega}'_jcc2jk)\\ &+\frac{1}{2\pi i}\sum_{j=1,\neq k,k-1}^{n}(\bar{\omega}_{j+1}cc6jk+\bar{\omega}_jcc5jk)\\ &+\frac{1}{2\pi i}\sum_{j=1,\neq k,k-1}^{n}(\bar{\omega}'_{j+1}cc8jk+\bar{\omega}'_jcc7jk)\\ &+\frac{1}{2\pi i}\bar{\omega}_k\ln\frac{z_{k+1}-z_k}{z_{k-1}-z_k}\end{aligned} \tag{38}$$

where $cc1jk$, $cc2jk$, $cc5jk$, $cc6jk$, $cc7jk$, and $cc8jk$ are functions of the geometry of the nodal points.

Let $\bar{\omega}_1 = \phi_1 + i\psi_1$ and define $c1$, $c2$, $c3$, and $c4$ as functions of nodal orientation; i.e., if $j \neq k$, $k-1$, then

$$\begin{aligned}c1jk &= cc1jk + cc6jk\\ c2jk &= -cc1jk + cc5jk\\ c3jk &= cc2jk + cc8jk\\ c4jk &= cc2jk + cc7jk\end{aligned} \tag{39}$$

if $j = k$ or $j = k-1$, then

$$\begin{aligned}c1jk &= cc1jk\\ c2jk &= -cc1jk\\ c3jk &= cc2jk\\ c4jk &= cc2jk\end{aligned}$$

If we now expand equation (38) and separate real and imaginary components, we obtain:

$$\begin{aligned}\phi_k \cong{}& \frac{1}{2\pi}\sum_{j=1}^{n}[\phi_{j-1}\mathrm{imag}(c1jk)+\psi_{j-1}\mathrm{real}(c1jk)]\\ &+\frac{1}{2\pi}\sum_{j=1}^{n}[\phi_j\mathrm{imag}(c2jk)+\psi_j\mathrm{real}(c2jk)]\\ &+\frac{1}{2\pi}\sum_{j-1}^{n}[\phi'_{j+1}\mathrm{imag}(c3jk)+\psi'_{j+1}\mathrm{real}(c3jk)]\\ &+\frac{1}{2\pi}\sum_{j-1}^{n}[\phi'_j\mathrm{imag}(c4jk)+\psi'_j\mathrm{real}(c4jk)]\\ &+\frac{1}{2\pi}\phi_k\mathrm{imag}\left(\ln\frac{z_{k+1}-z_k}{z_{k-1}-z_k}\right)\\ &+\frac{1}{2\pi}\psi_k\mathrm{real}\left(\ln\frac{z_{k+1}-z_k}{z_{k-1}-z_k}\right)\end{aligned} \tag{40}$$

$$\psi_k \cong \frac{-1}{2\pi}\sum_{j=1}^{n}[\phi_{j+1}\,\mathrm{real}(c1jk) - \psi_{j+1}\,\mathrm{imag}(c1jk)]$$
$$-\frac{1}{2\pi}\sum_{j=1}^{n}[\phi_j\,\mathrm{real}(c2jk) - \psi_j\,\mathrm{imag}(c2jk)]$$
$$-\frac{1}{2\pi}\sum_{j=1}^{n}[\phi'_{j+1}\,\mathrm{real}(c3jk) - \psi'_{j+1}\,\mathrm{imag}(c3jk)]$$
$$-\frac{1}{2\pi}\sum_{j=1}^{n}[\phi'_j\,\mathrm{real}(ck4jk) - \psi'_j\,\mathrm{imag}(c4jk)]$$
$$-\frac{1}{2\pi}\phi_k\,\mathrm{real}\left(\ln\frac{z_{k+1}-z_k}{z_{k-1}-z_k}\right)$$
$$+\frac{1}{2\pi}\psi_k\,\mathrm{imag}\left(\ln\frac{z_{k+1}-z_k}{z_{k-1}-z_k}\right) \qquad (41)$$

where real(c) and imag(c) indicate the real and imaginary components of a complex constant c. An exactly analogous procedure can be performed to obtain a similar representation for ϕ'_k and ψ'_k.

Discussion

Several ideal fluid flow problems have been solved by the previously developed CVBEM models. Results show similar model efficiencies between the different trial function techniques, and the error analysis which was based on the approximate boundary technique[2] shows relatively consistent results for all the CVBEM models considered.

Model efficiency

Most of the simple ideal fluid flow problems can be formulated by either a complex polynomial function or a Laurent series representation. A CVBEM model based upon a parabolic or cubic trial function obviously provides more accuracy than the linear trial function model when the problem solution is a complex polynomial (such as ideal fluid flow around a corner; i.e., $\omega = z^2$). Model efficiency of other ideal fluid flow problems with nonpolynomial solutions (such as ideal flow over a cylinder; i.e., $\omega = z + z^{-1}$) can be modestly improved by the higher-order trial function CVBEM models.

Overall, the CVBEM model based on a linear trial function shows comparable results to the other higher-order trial function models. The advantage of using the higher-order trial functions is that precise boundary conditions (e.g., the derivative terms of potential or stream function) can be handled more precisely.

Error analysis

The approximate boundary error analysis for the CVBEM is developed by Hromadka.[2]

Approximation error occurs due to the approximation function $\hat{\omega}(z)$ not satisfying the boundary conditions on the boundary Γ exactly. However, an approximate boundary $\hat{\Gamma}$ can be developed which represents the location where $\hat{\omega}(z)$ equals the specified boundary conditions such as level curves. Consequently, the CVBEM approximation error can be interpreted as a transformation of $\Gamma \rightarrow \hat{\Gamma}$ where the ultimate objective is to have $\hat{\Gamma}$ coincide with Γ. As $\hat{\Gamma}$ approaches Γ geometrically, the analyst is assured by the maximum modulus theorem that the maximum approximation error occurs on Γ and that the governing partial differential equation (Laplace) is solved exactly. Consequently, the final product is the exact solution for a problem geometry, which is the construction tolerance for the prototype construction.

Generally, the types of numerical approximation errors in solving potential problems are of two forms: errors due to not satisfying the (i) governing equation over Ω and (ii) boundary conditions continuously on Γ. For the CVBEM (and for other boundary integral equation methods), the first type of approximation error is eliminated due to both $\hat{\phi}$ and $\hat{\psi}$ being potential functions. But $\hat{\omega}(z)$ does not usually satisfy the boundary conditions continuously on Γ (if it did, then $\hat{\omega}(z) = \omega(z)$). The next step in the CVBEM analysis is to work with $\hat{\omega}(z)$ in order that $\hat{\omega}(z) \rightarrow \omega(z)$. The easiest form of error to study is the development of an approximate boundary $\hat{\Gamma}$ which represents the location where $\hat{\omega}(z)$ achieves the problem boundary conditions of $\omega(z)$.

For all test problems, the approximate boundary was developed for all the CVBEM models, and resulted in comparable accuracy in matching the problem geometry between each model. *Figure 5* depicts the streamlines and equipotential lines for ideal fluid flow over a cylinder. The approximate boundary of the cylinder is shown as the dashed line by the linear trial function model. Comparable accuracy of the approximate boundary was also observed for the higher-order trial function models considered.

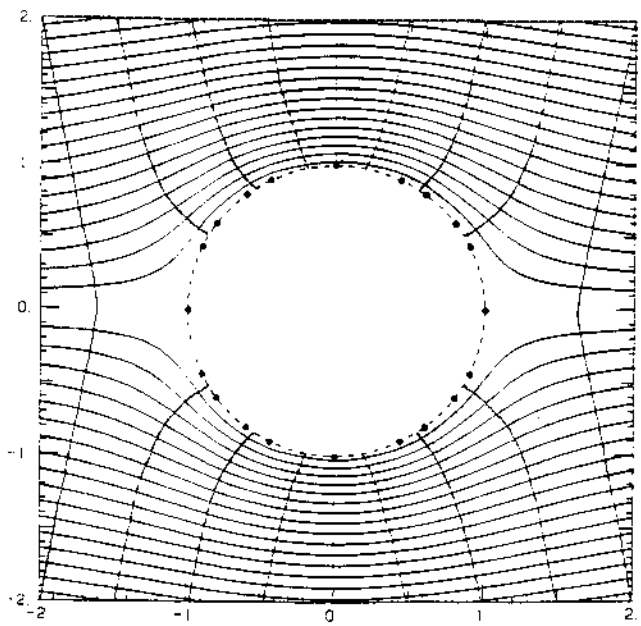

Figure 5 Flow field and approximate boundary for ideal fluid flow over a cylinder by linear CVBEM model

Conclusions

Nodal point equations are developed for the principal value of the Cauchy integral for the CVBEM by using the linear, parabolic, cubic, and Hermite cubic polynomial trial functions for interpolation. The nodal point equations provide the information needed for developing computer programs for each of the trial function interpolation techniques used with the CVBEM. Upon comparing the computational accuracy afforded by each of the four considered trial function techniques, we conclude that all four techniques provide approximately the same relative level of accuracy for problems which have potential solutions that are not finite-order complex polynomials.

Acknowledgments

The authors wish to acknowledge the Computational Hydrology Institute, Santa Rosa, California, USA, for its financial support during this research project. Also acknowledged is the applied mathematics program at California State University, Fullerton, California, USA, which provided the research resources needed to conclude this project.

References

1 Hromadka II, T. V. *Topics in Boundary Element Research*, Vol. 3, *Computational Aspects*, Chapter 7, *Complex Variable Boundary Elements*, Springer-Verlag, 1987

2 Hromadka II, T. V. *The Complex Variable Boundary Element Method*. Springer-Verlag, 1984